Experimental study of an all-fiber laser actively mode-locked by standing-wave acousto-optic modulation

**C. Cuadrado-Laborde · A. Díez · J.L. Cruz ·
M.V. Andrés**

Abstract We report an experimental study of an actively mode-locked erbium-doped all-fiber laser, based on a standing-wave acoustically-induced superlattice modulation. Our experiments involve the characterization of the laser as a function of the active fiber length, and with different types of delay line fibers. The effect of the modulation on the laser performance was also investigated. Narrower pulses were obtained at higher modulation depths, normal dispersion, and shorter lengths of active fiber. Optical pulses of 160 mW peak power and 630 ps temporal width were obtained at 9 MHz repetition rate.

1 Introduction

Mode-locked lasers can generate short light pulses either using passive or active approaches. Whenever we are interested in the generation of very short light pulses, i.e. in the femtosecond regime, passive mode-locking is the preferred technique [1, 2]. However, the saturable absorbers employed in passively mode-locked fiber lasers are sensitive to environmental changes, resulting in unstable output characteristics. On the contrary, active mode-locking operation results in longer but more stable light pulses, and they can easily be synchronized to a master clock. There are several reasons to prefer an all-fiber configuration for mode-locked lasers;

these are related with alignment-free sensitivity, compactness, and higher power efficiency, among other advantages. Besides this, an optical fiber is particularly suitable to form the cavity of a mode-locked laser, not only because it makes it possible to form a low-loss cavity, but also the dispersion of the cavity becomes easily adjustable by using fibers with different group velocity dispersions. This last point deserves particular attention in mode-locking fiber lasers, since it has been shown that there is a strong dependence of the output light pulses on the overall dispersion of the cavity, especially for very short pulses. Many of the benefits of using an all-fiber cavity would be lost if bulk components as electro-optic or acousto-optic modulators were used, since the use of bulk intracavity elements may cause degradation of the beam quality and high cavity losses. These features decrease the overall performance of the laser, often forcing one to the use of higher pump powers. Moreover, bulk components require fine alignment and good mechanical stability, which makes the design of practical systems rather demanding. Very few all-fiber approaches have been reported [3–7]. Among them, we have recently developed an actively mode-locked all-fiber laser, using a simple and low-insertion-loss modulation technique, which is based on standing-wave acoustically-induced superlattice modulation of a fiber Bragg grating [7]. Now, it is our purpose to show the behavior of this laser under different configurations, not only to gain physical insight into the dynamics of this kind of laser, but also looking towards an improvement of its performance. The output light pulses were analyzed as a function of the acoustically-induced modulation, the overall dispersion of the cavity, and the length of active fiber. Practical mechanisms for further narrowing of the optical pulses are also discussed.

C. Cuadrado-Laborde (✉) · A. Díez · J.L. Cruz · M.V. Andrés
Departamento de Física Aplicada y Electromagnetismo, ICMUV, Universidad de Valencia, C/ Dr. Moliner 50, 46100 Burjassot, Valencia, Spain
e-mail: Christian.Cuadrado@uv.es

C. Cuadrado-Laborde
Centro de Investigaciones Ópticas (CONICET La Plata-CIC), P.O. Box 3, 1897 Gonnet, Buenos Aires, Argentina

2 Laser setup and amplitude modulator

The setup of our mode-locked laser is schematically illustrated in Fig. 1. The gain was provided by an erbium-doped fiber (EDF) containing 300 parts per million (ppm) of Er^{3+}, with a cut-off wavelength of 939 nm, and a numerical aperture of 0.24. The active fiber was pumped through a WDM coupler by a pigtailed laser diode emitting at 976 nm, providing a maximum pump power of 160 mW. The acousto-optically modulated fiber Bragg grating (AOM-FBG), and a short delay line followed by a second fiber Bragg grating FBG_2, were fusion-spliced at each end of the active fiber, forming a Fabry-Pérot cavity.

The details of the AOM-FBG were reported in a previous work [7], so here we just recall its main features. It is composed of an RF source, a piezoelectric disk, a silica horn, and a fiber Bragg grating (FBG_1). The tip of the silica horn—which was fusion-spliced to the grating—launches longitudinal acoustic waves in the MHz range, causing new reflection bands to appear symmetrically at both sides of the original Bragg wavelength [8, 9]. By clamping the end of FBG_1, opposite to the silica horn, a standing acoustic wave is created and the sidebands rise and fall at twice the frequency of the acoustic wave. In this regime the AOM-FBG behaves as an amplitude modulator, which operates at twice the frequency of the electric signal used to drive the piezoelectric.

The delay line length (see Fig. 1) was selected to match the cavity round-trip time with the reciprocal of the optical modulation frequency, $2L = c/n2\nu_{PZT}$, where ν_{PZT} is the electrical frequency applied to the piezoelectric, c the speed of light in vacuum, n the modal index ($n = 1.447$), and L the cavity length. Since we used a piezoelectric with a resonance frequency of 5 MHz, the operation was limited to frequencies around this value. Finally, a translational stage was also necessary for matching the reflection band of FBG_2 to the short wavelength sideband of FBG_1, i.e. 1530.5 nm.

All the results reported here have been obtained exciting the piezoelectric disk with a frequency $\nu_{PZT} = 4.55$ MHz, and this corresponds to a cavity length of 11.4 m (in any case, fine tuning of ν_{PZT} is required within ± 10 kHz to obtain optimum mode-locking).

3 Experimental characterization

3.1 The dependence with the modulation voltage

The intensity of the reflection sidebands of the AOM-FBG can be dynamically controlled by varying the voltage applied to the piezoelectric. This voltage controls the amplitude of the propagating acoustic wave and the amplitude of the standing wave, as a function of the reflection at the clamp. Thus, the reflectivity of the sidebands (R) and the modulation depth are intrinsically linked, although the ratio is not linear. Figure 2(a) gives R and δR_{pp} ($\delta R_{pp} = (R_{Max} - R_{Min})/R_{Max}$, i.e. the relative peak-to-peak modulation amplitude of R) as a function of the voltage. In the
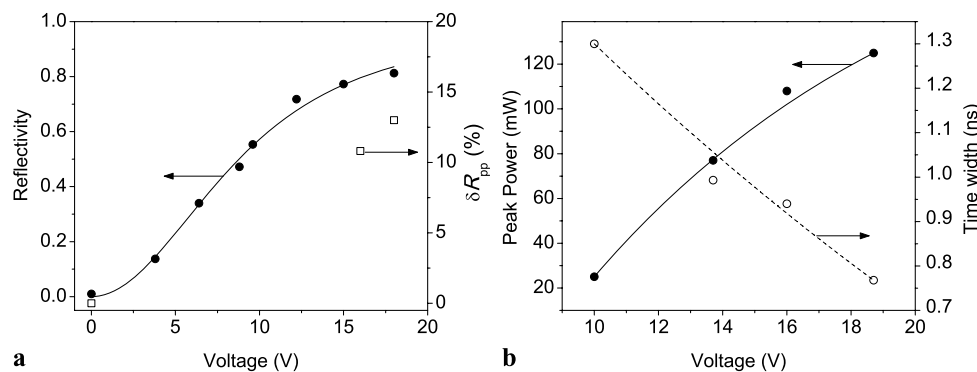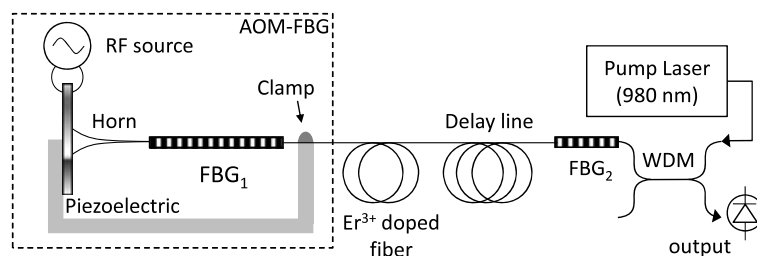

Fig. 1 Mode-locked fiber-laser setup

Fig. 2 (**a**) Measured reflectivity of the short wavelength sideband (*solid scatter points*)—together with its corresponding theoretical fitting (*solid curve*)—, and the peak-to-peak modulation amplitude (*open scatter points*) as a function of the voltage applied to the piezoelectric. (**b**) Peak power and time width of the output light pulses as a function of the voltage applied to the piezoelectric. Pump power of 160 mW

range of voltage available in our experimental setup, between 0 and 18 V, when the applied voltage increases, both the reflectivity and the modulation amplitude increase. Figure 2(b) shows the results corresponding to the first laser configuration, which involved 1.5 m of EDF, a delay line made of Corning LEAF optical fiber. Figure 2(b) shows the peak power and time width, respectively, as a function of the voltage applied to the piezoelectric. At lower reflectivities and modulation amplitudes, the peak power diminishes, whereas the time width increases. This is consistent with previous theoretical models of active mode-locking lasers, in which the time width is inversely related with both, the modulation depth and the reflectivity [1, 10]. From Fig. 2, one can conclude that further increase of the voltage might improve the pulse parameters, but it is not likely to lead to a great enhancement in terms either of peak power or temporal width, since the reflectivity is reaching the maximum and, in fact, some saturation in the peak power can be observed. However, an additional narrowing of the light pulses could be achieved if higher modulation depths were produced by a higher acoustic reflection from the clamp (see Fig. 1). At present the reflection coefficient produced by the clamp can be estimated to be less than 27%, so there is margin for a large improvement of the clamping technique. In addition, a higher efficient acousto-optic interaction could be achieved by writing the Bragg grating in the waist of a previously tapered section of a photosensitive fiber or by chemical etching of the cladding, since the reduction of the cross section of the fiber leads to an enhancement of the acoustic power. Figure 3(a) shows a train of mode-locked pulses, generated at twice the frequency of the electric signal that excites the piezoelectric. Figure 3(b) shows a detail of a single optical pulse, which was best fitted by a sech^2 type function (also shown). The best pulses obtained in this series of measurements had 125 mW peak power and 780 ps temporal width, see Fig. 2(b).
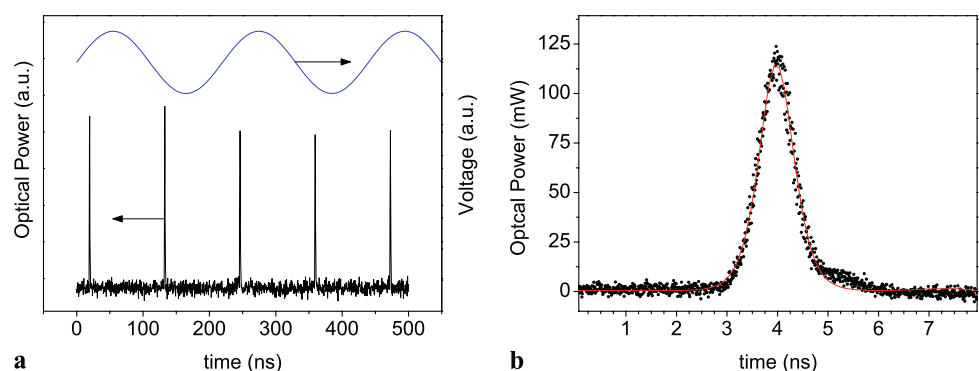
3.2 Configurations with different delay lines

In this section we summarize the operation of the laser when the fiber that forms the delay line is changed. Be-fore, the strong influence that dispersion has on the behavior of mode-locking lasers [1, 2, 10–12] has been recognized. Thus, we have paid special attention to this parameter and we have measured the characteristics of the pulses when changing the dispersive properties of the cavity. Figure 4 shows a dispersion map for every case studied in this work: Fig. 4(a–c) corresponding to this subsection, and Fig. 4(d–e) corresponding to Sect. 3.3. In this way, the different kinds of dispersions that light pulses experience through its build up within the cavity can be easily followed, as well as its average value. The dispersion for each type of optical fiber used throughout this work was measured by the frequency-domain modulated-carrier method. Figure 4(a) shows the dispersion map for the cavity studied in previous Sect. 3.1. It is composed of three different types of fiber, with the following dispersions: Fibercore SM980 ($D = -4.09$ ps/nm/km), EDF ($D = -18.8$ ps/nm/km), and Corning LEAF ($D = 2$ ps/nm/km), which corresponds to the pigtails of the FBGs, the active fiber, and the delay line, respectively. Thus, the resulting average dispersion of this cavity is normal and its value is -1.2 ps/nm/km. According to previous theoretical models [12], this being a dispersion-mixed cavity, a sech^2 function for the light pulses is expected, as is depicted in Fig. 3(b). Further, it was shown that soliton propagation can even be formed in the normal dispersion regime also. As soliton formation is induced purely by the existence of gain, the soliton was named a gain-guided soliton [13].

Next, the optical fiber of the delay line—the Corning LEAF fiber—was replaced by a normal dispersion fiber—Fibercore SM980—, leading to a higher (normal) overall dispersion of -5.8 ps/nm/km, see Fig. 4(b). Figure 5 shows the peak power and time width of both configurations, i.e. the cavities with the LEAF and the SM980 delay lines, as a function of the pump power. With the new delay line, a higher pump reaches the EDF, since a better effective area compatibility is insured throughout the different fibers of the system—in fact, unlike LEAF fiber, the SM980 insures single-mode propagation of the pump power. As a result, output pulses have higher peak power and shorter time width than in the previous configuration.

Fig. 3 (**a**) Mode-locked train of pulses generated at 9.1 MHz repetition rate with 160 mW of pump power, and modulation voltage of 4.55 MHz and 18 V peak-to-peak. (**b**) A single pulse and its corresponding fitting by a sech^2 function (*scatter points* and *solid curve*, respectively)
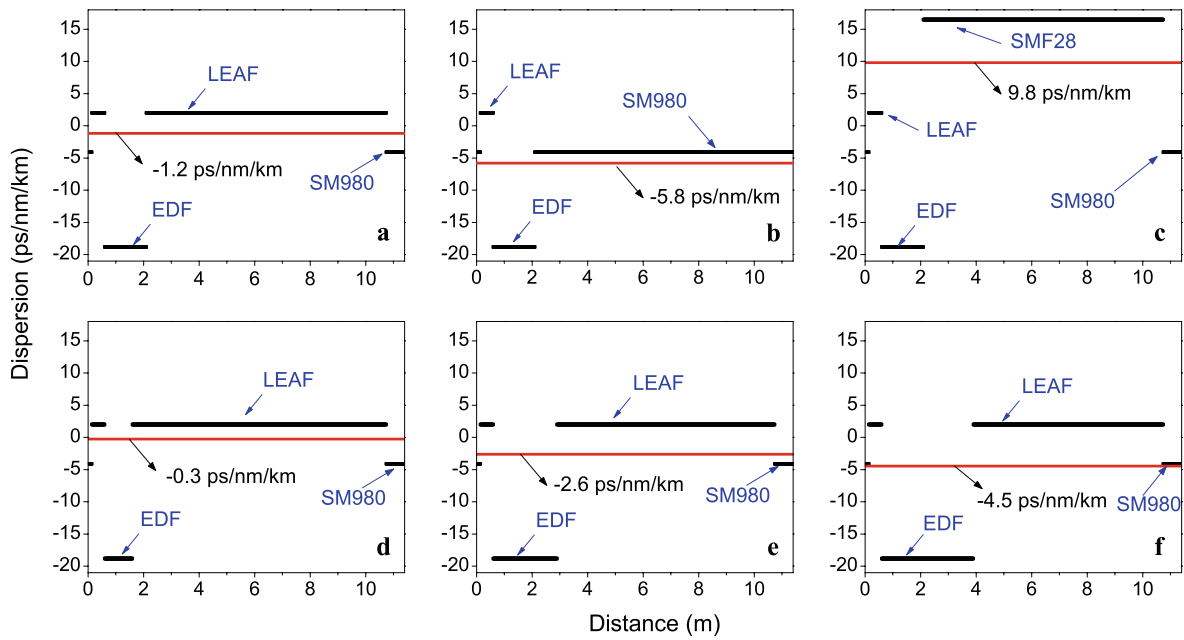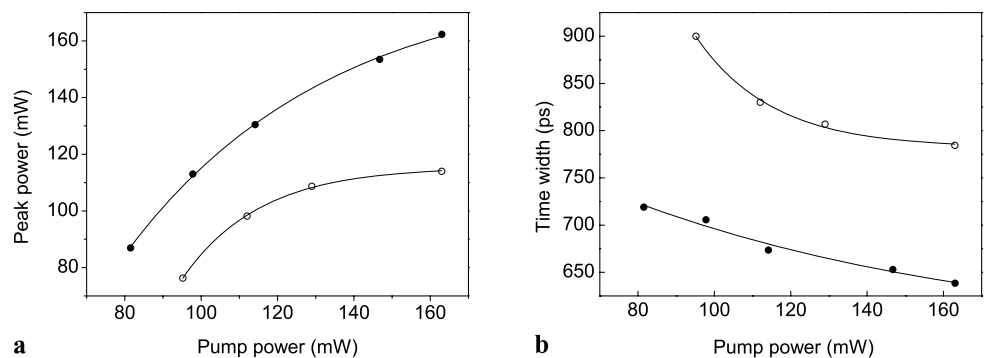
Fig. 4 Dispersion maps of the laser. (**a–c**) Using three different optical fibers as delay line, with a constant length of EDF $L_{EDF} = 1.5$ m: (**a**) LEAF, (**b**) SM980, and (**c**) SMF28. (**d–f**) Keeping the same delay line (LEAF) and changing the length of EDF: (**d**) $L_{EDF} = 1$ m, (**e**) $L_{EDF} = 2.3$ m, and (**f**) $L_{EDF} = 3.3$ m. In all cases the *red line* represents the average dispersion of the cavity

Fig. 5 Peak power and time width of the output light pulses, (**a**) and (**b**) respectively, as a function of the pump power for two different delay lines: LEAF (*open circles*) and SM980 (*solid circles*)
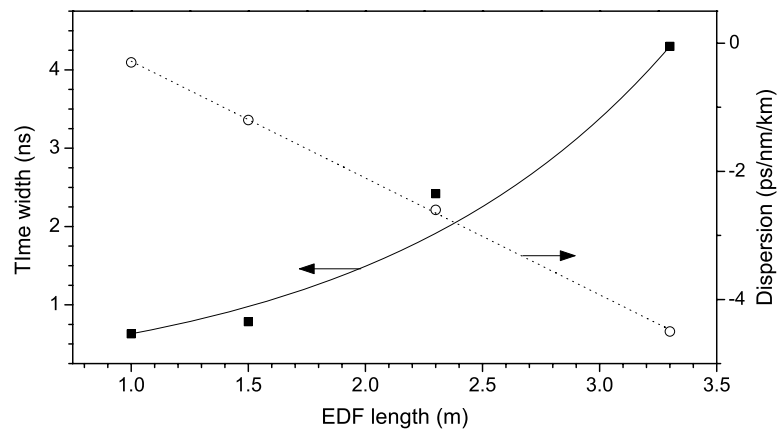
In this way, optical pulses with temporal width and peak power of 640 ps and 160 mW, respectively, were obtained. These pulse parameters represent an improvement of 18% and 28% with respect to the previous configuration. Finally, in order to reverse the sign of the average dispersion of the cavity, we used an SMF28 optical fiber for the delay line, resulting in an average—anomalous—dispersion of 9.8 ps/nm/km, see Fig. 4(c). In this case, we did not observe mode-locking lasing. One reason for this could be the large average dispersion introduced within the cavity, since mode-locking fiber lasers usually work with a lower average dispersion.

3.3 The dependence with the EDF length

The change of the pulse parameters was measured as a function of the length of EDF—ranging from 0.5 to 3.3 m—,

but keeping a constant cavity length of 11.4 m, by adjusting each time the length of LEAF fiber. Figures 4(a, d–f) show the dispersion maps for each case. It can be observed that—regardless of the amount of EDF used—the overall dispersion remains normal. The temporal pulse width as a function of the EDF length is shown in Fig. 6, for a fixed pump power of 160 mW. This figure includes the average dispersion of the cavity as a function of the EDF length. A direct relationship can be observed between the EDF length, the dispersion, and the time width of the pulses, with a minimum of 630 ps obtained for an EDF length of 1 m. This kind of interplay between gain and time width agrees with the theoretical results given by Kuizenga and Siegman for homogeneously broadened actively mode-locked lasers [10]. Further narrowing of the optical pulses could not be reached by this way, since no mode-locking lasing was observed with

Fig. 6 Time width of the output light pulses, as a function of the EDF length, for a fixed pumping power of 160 mW. Additionally, the average dispersion of the cavity is also shown for each EDF length

0.5 m of EDF and the available pump power, as a result of insufficient cavity gain.

4 Conclusion

In this work we have carried out an experimental study of an all-fiber actively mode-locked laser under different configurations. We have studied the peak power and temporal width of the optical pulses as a function of the acoustically-induced modulation, different types of delay lines, and changing the length of EDF. The effects of the overall cavity dispersion and the net gain have been discussed and some alternatives for further improvement of the laser operation have been identified.

References

1. H.A. Haus, IEEE J. Sel. Top. Quantum Electron. **6**, 1173 (2000)
2. M. Nakazawa, J. Opt. Fiber. Commun. Rep. **2**, 462 (2005)
3. D.O. Culverhouse, D.J. Richardson, T.A. Birks, P.St.J. Russell, Opt. Lett. **20**, 2381 (1995)
4. M.Y. Jeon, H.K. Lee, K.H. Kim, E.H. Lee, W.Y. Oh, B.Y. Kim, H.W. Lee, Y.W. Koh, Opt. Commun. **149**, 312 (1998)
5. N. Myren, W. Margulis, IEEE Photonics Technol. Lett. **17**, 2047 (2005)
6. M.W. Phillips, A.I. Ferguson, G.S. Kino, D.B. Patterson, Opt. Lett. **14**, 680 (1989)
7. C. Cuadrado-Laborde, A. Diez, M. Delgado-Pinar, J.L. Cruz, M.V. Andrés, Opt. Lett. **34**, 1111 (2009)
8. W.F. Liu, P.St.J. Russell, L. Dong, Opt. Lett. **22**, 1515 (1997)
9. W.F. Liu, P.St.J. Russell, L. Dong, J. Lightw. Technol. **16**, 2006 (1998)
10. D.J. Kuizenga, A.E. Siegman, IEEE J. Quantum Electron. **6**, 694 (1970)
11. F. Shohda, T. Shirato, M. Nakazawa, K. Komatsu, T. Kaino, Opt. Express **16**, 21191 (2008)
12. P.A. Bélanger, Opt. Express **13**, 8089 (2005)
13. L.M. Zhao, D.Y. Tang, J. Wu, Opt. Lett. **31**, 1788 (2006)